Thermal excitation of the Co^{3+} triplet spin-state in $LaCoO_3$ determined by polarized neutron diffraction

2006 J. Phys.: Condens. Matter 18 3517

(http://iopscience.iop.org/0953-8984/18/13/019)

INSTITUTE OF PHYSICS PUBLISHING JOURNAL OF PHYSICS: CONDENSED MATTER

J. Phys.: Condens. Matter **18** (2006) 3517–3525 doi:10.1088/0953-8984/18/13/019

Thermal excitation of the Co^{3+} triplet spin-state in $LaCoO_3$ determined by polarized neutron diffraction

V P Plakhty[1,5], P J Brown[2], B Grenier[3], S V Shiryaev[4], S N Barilo[4], S V Gavrilov[1] and E Ressouche[3]

[1] Petersburg Nuclear Physics Institute, 188300, Gatchina, St Petersburg, Russia
[2] Institut Laue-Langevin, 38042 Grenoble Cedex 9, France
[3] CEA-Grenoble, DFMC/SPSMS/MDN, 38042 Grenoble Cedex 9, France
[4] Institute of Solid State and Semiconductor Physics, 22072, Minsk, Belarus

E-mail: plakhty@pnpi.spb.ru

Received 23 September 2005, in final form 10 February 2006
Published 17 March 2006
Online at stacks.iop.org/JPhysCM/18/3517

Abstract

The magnetic moment induced by an external magnetic field of 5.8 T on the Co^{3+} ions in $LaCoO_3$ has been measured by polarized neutron diffraction. Measurements were made at 100 K, near to the susceptibility maximum usually associated with a gradual spin-state transition, as well as at 1.5 and at 285 K. The data give evidence for a transition from the ground singlet state ($S = 0$) to the excited triplet intermediate spin-state ($S = 1$). The energy of $\Delta_H \approx 1000$ K estimated for the high-spin-state ($S = 2$), is too high to make a significant contribution to the moment, even at $T = 285$ K. There is evidence for a small negative spin density associated with the oxygen ligands in agreement with the theory that predicts intermediate spin as the first excited state.

1. Introduction

Competition between intra-atomic exchange and the crystal field results in three possible states for Co^{3+} ions in solids: the ground low-spin-state (LS, $t_{2g}^6 e_g^0$, $S = 0$) and the excited states with intermediate spin (IS, $t_{2g}^5 e_g^1$, $S = 1$) and high spin (HS, $t_{2g}^4 e_g^2$, $S = 2$) [1]. The small energy differences between these states leads to the quite unusual magnetic properties of $LaCoO_3$. Although this material has been extensively studied during the last 40 years, the nature of the lowest energy excited spin-state remains unclear. The magnetic susceptibility of $LaCoO_3$ is negligible at temperatures $T < 50$ K, goes through a maximum around 100 K and then decreases following the Curie–Weiss law to a plateau in the range 400 K $< T <$ 600 K [2]. The effective moments of the Co^{3+} ions calculated from the susceptibility data [2, 3] are $M \approx 2\ \mu_B$ at $T \approx 100$ K and $M \approx 3.5\ \mu_B$ at $T \approx 900$ K. No long-range magnetic order has been found in

[5] Author to whom any correspondence should be addressed.

all the temperature range where $M \neq 0$ [4, 5], although short-range ferromagnetic correlations have been observed in neutron polarization analysis experiments [6]. The susceptibility maximum at 100 K was originally thought to arise from the LS–HS transition [7]. (Here a spin-state transition is not a phase transition in conventional sense. It is a gradual transition in which the relative populations of two energy levels change due to thermal excitation.) The insulating properties below 400–600 K were attributed to NaCl-type ordering of LS and HS Co^{3+} ions [8]. However, this latter hypothesis is not supported by neutron diffraction studies [9].

A completely different approach [10] has been made based on the observation that oxides with formally high oxidation states may be negative charge-transfer systems. For Co^{3+} a relatively stable hole state on the ligand ions, with the hole spin being opposite to that of the Co^{3+}, favours an IS first excited state [11, 12]. The IS state has the configuration $t_{2g}^5 e_g^1$, in which the double degeneracy of the e_g orbitals is lifted by the Jahn–Teller effect. In the rhombohedral lattice containing two Co ions per unit cell, 'antiferro' orbital ordering of the half-filled orbitals, for instance y^2–z^2, yz and x^2–y^2, xy, minimizes the Coulomb interaction between e_g and t_{2g} electrons [10]. Such ordering could account for the lack of metallic conduction in the range $100\ \text{K} < T < 500\ \text{K}$. According to [10], the broad semiconductor-to-metal transition around 500 K is associated with gradual orbital disordering of IS state ions, with the transition to the HS state taking place at yet higher temperature. This idea that the anomalous magnetic and thermal behaviour is due to a LS–IS transition accompanied by orbital ordering has motivated a number of recent experiments. Magnetic susceptibility and thermal expansion [13], susceptibility, photoemission spectroscopy and x-ray absorption spectroscopy [14], electron spin resonance data [15] and structural properties [16, 17] are all in reasonable agreement with the model [10]. The agreement can be improved by introducing further parameters: for instance, a three-level model with a varying population of LS, IS and HS states has been explored in [16] to describe both structural and magnetic data. The phonon modes in [18] were interpreted in terms of a dynamical Jahn–Teller effect in the thermally excited IS state. A cooperative Jahn–Teller distortion associated with e_g orbital ordering [10] was later demonstrated by high-resolution x-ray diffraction [19]; the space group symmetry was shown fall from $R\bar{3}c$ to its monoclinic sub-group $I2/a$ on heating through $T \approx 100$ K. However, discussion is still going on about whether the first excited state is IS or HS.

It is clear that an important point to understand, independently of the identity of the excited state, is the lack of long-range magnetic order above the spin-state transition. The experimental data on both the magnetic susceptibility and specific heat of $LaCoO_3$ can be accounted for if the spin-state excitation is assumed to reduce the exchange interaction [20]. This effect is supposed to originate from a difference in the covalence between Co–O bonds formed by low-spin and excited-spin Co^{3+} ions. Six models involving mixtures of IS and HS states with different degeneracy and g-factors were tested in [20]. Whilst all models could reproduce the magnetic susceptibility up to 300 K, the specific heat data up to 100 K could be accounted for by an exited state corresponding to only one of the IS + HS mixtures [20].

Polarized neutron diffraction [21] allows the local magnetization on the Co^{3+} ion and the O^{2-} ligand to be measured independently, whereas bulk magnetometry just gives their sum. The first objective of our experiment was to measure the field-induced moment on the Co^{3+} ion in the vicinity of the broad susceptibility maximum at $T \approx 100$ K caused by the gradually increasing population of the first excited state. This moment value, m (100 K), can be used for calculating the gaps Δ_I and Δ_H from the ground LS state to the IS and HS states, respectively. The gaps thus obtained should be close to 100 K, which provides a criterion for choosing between the IS and HS states. The possibility that the absence of long-range magnetic ordering is due to a negative cooperative effect [20] can be addressed by measuring any field-induced moment on the oxygen O^{2-} ligand at $T = 100$ and 285 K.

2. Polarized neutron diffraction and its application to $LaCoO_3$

The intensity of unpolarized neutrons scattered by a Bragg reflection with scattering vector **k** from a crystal with ordered magnetic moments can be expressed as

$$I(\mathbf{k}) \propto |F_N|^2 + |\mathbf{M}_\perp|^2, \tag{1}$$

where

$$\mathbf{M}_\perp = \mathbf{k} \times \mathbf{F}_M \times \mathbf{k}. \tag{2}$$

The nuclear, F_N, and magnetic, $\mathbf{F}_M$, structure factors are given in terms of the coordinates $\mathbf{r}_i$ of atoms in the unit cell, their nuclear scattering lengths b_i, their magnetic moments $\mathbf{m}_i$ and magnetic form-factors $f_i(\mathbf{k})$ as

$$F_N = \sum_i b_i \exp(i\mathbf{k} \cdot \mathbf{r}_i), \tag{3}$$

$$F_M = \sum_i \mathbf{m}_i f(\mathbf{k}) \exp(i\mathbf{k} \cdot \mathbf{r}_i). \tag{4}$$

For neutrons with initial polarization **P** parallel to the applied field the corresponding intensity $I^+(\mathbf{k})$ is expressed as

$$I^+(\mathbf{k}) \propto |F_N|^2 + 2\,\mathrm{Re}(F_N^*(\mathbf{P}\mathbf{M}_\perp)) + |\mathbf{M}_\perp|^2. \tag{5}$$

When the structure is centrosymmetric and the magnetic moments are aligned parallel to **P** by a magnetic field, F_N and $\mathbf{F}_M$ are real. If the ratio between the magnetic and nuclear structure factors is γ, the unpolarized intensity $I(\mathbf{k}) \propto 1 + \gamma^2$ and the flipping ratio R between the intensities of neutrons with polarization parallel and antiparallel to the applied field is

$$R = \frac{I^+}{I^-} = \frac{|F_N|^2 + 2F_N\mathbf{P} \cdot \mathbf{M}_\perp + |\mathbf{M}_\perp|^2}{|F_N|^2 - 2F_N\mathbf{P} \cdot \mathbf{M}_\perp + |M_\perp|^2} = \frac{1 + 2P\gamma + \gamma^2}{1 - 2P\gamma + \gamma^2}. \tag{6}$$

When γ is small the contribution of magnetism to the unpolarized intensity is proportional to γ^2, whereas its contribution to R is proportional to $4P\gamma$. Measurements of the flipping ratio therefore make it possible to determine very small magnetic moments such as those induced by an external field in a paramagnetic crystal.

According to a recent neutron diffraction study [17], the structure of $LaCoO_3$ in the temperature range $5 \leqslant T\ (\mathrm{K}) \leqslant 1000$ is that of the rhombohedrally distorted perovskite with space group $R\bar{3}c$. The rhombohedral unit cell, with edges $\mathbf{a}_R$, $\mathbf{b}_R$ and $\mathbf{c}_R$, shown in figure 1, contains two perovskite cells with edges $\mathbf{a}_C$, $\mathbf{b}_C$, $\mathbf{c}_C$, orientated so that $\mathbf{a}_R = \mathbf{a}_C + \mathbf{b}_C$, $\mathbf{b}_R = \mathbf{b}_C + \mathbf{c}_C$ and $\mathbf{c}_R = \mathbf{c}_C + \mathbf{a}_C$. In the hexagonal description of the rhombohedral cell, which is that used in the rest of this paper, the cell edges are $\mathbf{a}_H = \mathbf{a}_C - \mathbf{c}_C$, $\mathbf{b}_H = -\mathbf{a}_C + \mathbf{b}_C$, $\mathbf{c}_H = 2\mathbf{a}_H + 2\mathbf{b}_H + 2\mathbf{c}_H$.

The doubling of the perovskite cell is exclusively due to antiparallel displacements of the oxygen atoms, as shown by the arrows in figure 1. This means that nuclear structure factors of reflections with $l = 2n+1$ are due entirely to the oxygen ions, whereas all the constituent atoms contribute to those with even l. The magnetic structure factors of the even-l reflections depend mainly on the magnetic moment on the Co ion but will also contain contributions from any moment on the oxygen ligands; those of the odd-l reflections arise only from the perturbation of the atomic magnetization due to the rhombohedral distortion.

The rhombohedral distortion is due to compression along one of the four body diagonals of the cubic perovskite cell. Any one of these diagonals may be chosen, resulting in four possible twins; the number of twins being equal to the ratio between the orders of the symmetric group $Pm3m$ (48) and its sub-group $R\bar{3}c$ (12). In the rhombohedral structure each reflection of the

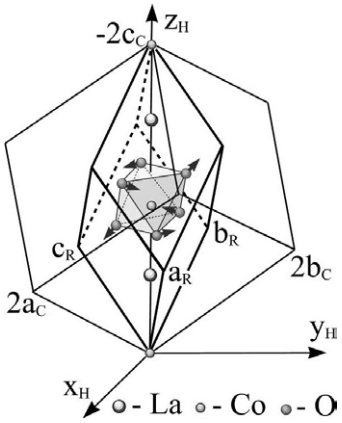

Figure 1. Unit cell of $LaCoO_3$. The explanations are given in the text.

perovskite cell $2\mathbf{a}_C$, $2\mathbf{b}_C$, $2\mathbf{c}_C$ splits into four parts, one from each twin with the three-fold axis along the space diagonals 1—[111], 2—[$\bar{1}$11], 3—[$\bar{1}\bar{1}$1], 4—[1$\bar{1}$1]. For the hexagonal setting used in our calculations, the indices of reflections (h_i, k_i, l_i) from the ith twin are expressed through those of the [111] one as $(h_i k_i l_i) = \hat{T}_i \cdot (h_1 k_1 l_1)$, where the matrices $\hat{T}_i$ are:

$$\hat{T}_1 = \begin{pmatrix} 1 & 0 & 0 \\ 0 & 1 & 0 \\ 0 & 0 & 1 \end{pmatrix}, \qquad \hat{T}_2 = \begin{pmatrix} -\frac{1}{3} & -\frac{2}{3} & \frac{1}{3} \\ 1 & 1 & 0 \\ -\frac{4}{3} & \frac{4}{3} & \frac{1}{3} \end{pmatrix},$$
$$\hat{T}_3 = \begin{pmatrix} -1 & 0 & 0 \\ \frac{2}{3} & \frac{1}{3} & \frac{1}{3} \\ \frac{4}{3} & \frac{8}{3} & -\frac{1}{3} \end{pmatrix}, \quad \hat{T}_4 = \begin{pmatrix} \frac{1}{3} & \frac{2}{3} & -\frac{1}{3} \\ -\frac{1}{3} & \frac{1}{3} & \frac{1}{3} \\ \frac{8}{3} & \frac{4}{3} & \frac{1}{3} \end{pmatrix}. \tag{7}$$

Since the distortion is small ($\alpha = 90.98°$ at room temperature) these four reflections cannot be resolved by neutron diffractometers with conventional resolution and the twinning must be taken into account in the data analysis. In particular, the twinning will invalidate the trigonal symmetry if the twin populations are not equal.

3. Crystal growth and characterization

Single crystals of $LaCoO_3$ were grown by an anodic electro-deposition technique [22] modified to use seeded flux melt growth based on a solvent consisting of a Cs_2MoO_4–MoO_3 mixture in the ratio 2.2:1 [23]. The material from which the crystals were to be grown was placed in a 100 cm^3 platinum crucible and an appropriate amount of the solvent added; a seed crystal served as the anode and the crucible itself as the cathode of the two-electrode electrochemical cell. The crystals were grown at a temperature of about (950–1000) °C under a current density of (0.5–0.7) mA cm^{-2}. A crystal of about 400 mg ($4 \times 4 \times 4$ mm^3) was chosen for the neutron diffraction experiment. With decreasing temperature its magnetic susceptibility goes through the wide maximum $\chi_{max} \approx 4 \times 10^{-3}$ emu mol^{-1} at $T \approx 100$ K, but, despite being in the LS state, it increases again at the lowest temperatures. This Curie-like behaviour at very low temperature has been reported in almost all the publications on $LaCoO_3$, for instance [13, 18, 20]. This anomalously high sample-dependent susceptibility is probably attributed either to the Co^{4+} cations ($S = 5/2$) due to some La vacancies [24], or to the surface

cobalt atoms [25]. The contributions of this component to the magnetization at the temperatures of the experiment, 100 and 285 K (6% and 4%, respectively), were estimated using the Curie law and are negligible in comparison with the experimental precision of the magnetic moments determined in the neutron diffraction experiment. A preliminary experiment to test the quality of the crystal and to verify the structural parameters was carried out at ambient temperature on the four-circle diffractometer D15 at ILL with wavelength $\lambda = 1.17$ Å and using a small 32×32 pixel multidetector. The reflections were rather wide and irregularly shaped, which limited the precision of integration; their full widths at half height varied from 2° to 5° of arc. The lattice parameters $a_H = b_H = 5.4639(9)$ Å, $c_H = 13.372(4)$ Å obtained at $T = 100$ K from refinement of the Bragg reflection positions are a little bigger than those from the powder diffraction experiment [17], but this may be due to the calibration of the wavelength. The integrated intensities were used in a least squares refinement to obtain the temperature factors and the coordinate of the oxygen atom. The measured intensities were assumed to contain contributions from all four rhombohedral twins, and the fractions of each twin component present were also refined. The value $x_O = 0.5523(5)$ was obtained for the oxygen position parameter in agreement with [17]. A small imbalance in the domain populations corresponding to fractions 0.230(8), 0.241(9), 0.286(9), 0.244(9) of the twins T_1–T_4 of equation (7) was present. No significant extinction was found.

4. Polarized neutron measurements

The flipping ratio measurements were made on the D23 polarized neutron diffractometer installed at the supermirror-coated thermal neutron guide H25 of the ILL high-flux reactor. D23 uses normal beam geometry with a detector which can be inclined to the horizontal plane. The crystal was mounted with its hexagonal axis [001] vertical and magnetized by a cryomagnet producing vertical field of 5.8 T. Polarized neutrons of wavelength $\lambda = 1.246$ Å were obtained by reflection from the (111) plane of a Heusler alloy monochromator. The flipping ratios of 61, 130 and 260 different Bragg reflections were measured at 1.5, 100 and 285 K, respectively; of these 26 were independent under the rhombohedral symmetry, 9 with $l = 2n + 1$ and 17 with $l = 2n$. Table 1 contains the data averaged over rhombohedrally equivalent reflections. In the final analysis these reflections were not averaged together in order to take into account the inequality found in the twin populations.

The flipping ratio of each reflection measured was used independently in a least squares refinement of the parameters of various possible models for the atomic magnetization in $LaCoO_3$. Four models of increasing complexity were tried. In the simplest the magnetization is modelled by the spherically symmetric distribution corresponding to a Co^{3+} ion [26] centred at each Co position; the only parameter fitted is the Co^{3+} moment. For the IS state of Co^{3+} the unpaired electron is in an e_g state and there is a hole in the t_{2g} manifold, so the corresponding magnetization should have e_g symmetry with respect to the cubic perovskite cell. In the second model the asphericity appropriate to such e_g symmetry is applied to the Co^{3+} magnetization at each site; again the only parameter fitted is the Co^{3+} moment. The third and fourth models are extensions of the first two in which a small moment with a distribution corresponding to that of the 2p electrons of the O^{2-} ion [24] resides on the oxygen sites. In these latter models two parameters, the Co^{3+} and O^{2-} moments, have been refined.

The least squares program calculates the flipping ratio for the model and its differentials with respect to the parameters by accumulating properly weighted contributions to the numerator and denominator of equation (6) calculated from all four twin components. The results obtained with the four models at 1.5, 100 and 285 K are given in table 2.

Table 1. Values of the flipping ratios R measured at temperatures of 1.5, 100 and 285 K and averaged over rhombohedrally equivalent reflections.

h	k	l	$\sin\theta/\lambda$	R (1.5 K)	R (100 K)	R (285 K)
1	1	0	0.1498	1.662(11)	1.106(4)	1.049(5)
2	1	−2	0.1982	0.92(6)	0.92(2)	0.95(3)
2	0	2	0.2247	0.911(2)	0.9799(14)	0.993(2)
2	2	0	0.2995	1.071(4)	1.012(3)	1.006(2)
3	0	0	0.3177	1.236(9)	1.045(3)	1.017(3)
3	2	−2	0.3265	0.890(14)	0.974(5)	0.996(11)
3	1	2	0.3745	1.03(5)	0.993(13)	1.00(2)
4	0	−2	0.4302	0.934(5)	0.985(3)	0.993(3)
4	1	0	0.4366	1.087(11)	1.024(4)	1.009(3)
3	3	0	0.4493	1.08(2)	1.007(5)	1.009(6)
4	3	−2	0.4677	0.97(2)	0.996(5)	1.002(11)
5	1	−2	0.5242	1.04(3)	1.006(8)	1.02(2)
4	2	2	0.5242	0.946(9)	0.993(3)	0.999(4)
5	0	2	0.5348	0.917(14)	0.983(8)	0.991(6)
5	2	0	0.5703	1.009(9)	1.002(2)	1.000(3)
6	0	0	0.6354	1.008(9)	1.005(3)	0.998(5)
6	1	2	0.6656	1.01(2)	0.999(9)	1.005(12)
2	1	1	0.2621	0.994(9)	0.996(4)	1.007(5)
1	1	3	0.2622	1.008(7)	0.998(4)	0.997(4)
3	1	−1	0.3199	1.000(5)	1.003(3)	1.001(4)
3	2	1	0.4119	1.00(6)	1.006(15)	1.00(2)
2	2	3	0.4119	1.009(8)	0.999(4)	0.997(4)
4	1	−3	0.4119	0.999(7)	0.995(4)	1.005(7)
4	2	−1	0.4509	0.998(7)	1.004(3)	1.001(3)
4	1	3	0.4868	1.004(9)	1.000(5)	0.998(6)
3	3	3	0.5617	0.994(14)	1.000(3)	1.004(5)

Table 2. Results obtained from least squares refinements of the flipping ratio for four models of the magnetization distribution in $LaCoO_3$ induced by a field of 5.8 T. The goodness of fit is defined in terms the observed flipping ratios $R_n^{\rm obs}$, their standard deviations σ_n and the calculated values $R_n^{\rm calc}$ as $\chi^2 = (N-M)^{-1}\sum_{n=1}^{N}\sigma_n^{-2}(R_n^{\rm obs}-R_n^{\rm calc})^2$, where N and M are the numbers of observations and variables, respectively.

T (K)	Parameter	Model 1[a]	Model 2[b]	Model 3[c]	Model 4[d]
	$m(Co^{3+})$, μ_B	0.52(6)	0.53(6)	0.41(12)	0.42(12)
1.5	$m(O^{2-})$, μ_B	—	—	−0.11(5)	−0.11(5)
	χ^2	56.5	56.6	43.5	43.7
	$m(Co^{3+})$, μ_B	0.129(8)	0.131(8)	0.10(2)	0.11(2)
100	$m(O^{2-})$, μ_B	—	—	−0.021(7)	−0.021(7)
	χ^2	3.81	3.83	3.19	3.23
	$m(Co^{3+})$, μ_B	0.056(4)	0.057(4)	0.052(9)	0.053(9)
285	$m(O^{2-})$, μ_B	—	—	−0.006(4)	−0.005(4)
	χ^2	1.88	1.90	1.84	1.86

[a] Spherically symmetric Co^{3+}.
[b] Co^{3+} with e_g symmetry.
[c] Spherically symmetric Co^{3+} and spherical O^{2-} 2p magnetization.
[d] Co^{3+} with e_g symmetry and spherical O^{2-} 2p magnetization.

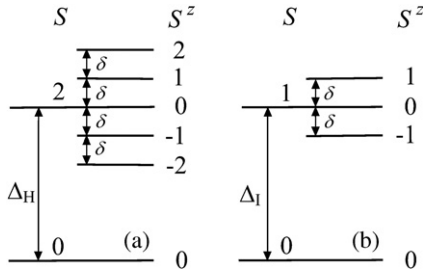

Figure 2. The level splitting for the HS state (a) and the IS state (b).

5. Results and discussion

The much larger χ^2 for the 1.5 K data refined with all the models may be explained by the use of the free atom cobalt 3+ form-factor in the model calculations, although the Co^{3+} is in the singlet state at this temperature, and the Curie-like component is probably due to a small number of Co^{4+} ions with $S = 5/2$ as has been discussed in section 3. More complex models of this kind have not been tried since we need this moment value only to make a small Curie law correction (6% and 2%) to the moments at $T = 100$ and 285 K, respectively. As seen from table 2, the standard deviation obtained at 1.5 K, even with the large χ^2 value, is sufficient for this purpose.

It can be seen that there is not much difference in the goodness of fit at the same temperature between the four models, although in all cases the best fit is obtained with model 3 in which the Co^{3+} moment is spherically symmetric and there is a small negative moment associated with oxygen. We shall use this result in further calculations. First, we compare the result with the macroscopic susceptibility data. For this purpose one should use the moment $M = m(Co^{3+}) + 3 \cdot m(O^{2-})$ taking into account the coordination number and that each ligand is shared between two Co ions. The susceptibility thus calculated, $\chi(100\ \mathrm{K}) = 4(2) \times 10^{-3}$ emu mol^{-1} and $\chi(285\ \mathrm{K}) = 3(1) \times 10^{-3}$ emu mol^{-1}, is in agreement with the magnetometry data, $\chi(100\ \mathrm{K}) = (4.2\text{–}4.3) \times 10^{-3}$ emu mol^{-1} and $\chi(285\ \mathrm{K}) = (3.3\text{–}3.4) \times 10^{-3}$ emu mol^{-1} of this work and [13, 18, 20].

The magnetization $m(T)$ of the Co^{3+} ion corrected for the Curie-like contamination measured at 1.5 K results in the following:

$$m\ (100\ \mathrm{K}) = 0.09(1)\ \mu_\mathrm{B}, \qquad m\ (285\ \mathrm{K}) = 0.050(9)\ \mu_\mathrm{B}. \tag{8}$$

These moment values have been used to calculate the gaps Δ_I and Δ_H, from the ground LS state to the IS and HS states, respectively. The gaps are shown in figure 2, together with the level splitting in an external magnetic field H in multiples of $\delta = g\mu_\mathrm{B}H$. As mentioned in section 1, the gap obtained from m (100 K), near to the spin-state transition, should be close to 100 K and this criterion can be used to choose which of the two proposed spin-states is excited at $T \approx 100$ K.

One can calculate $m(T)$ as

$$m(T) = -g\mu_\mathrm{B}S\nu \mathrm{e}^{-\Delta/T}\left\{\sum_i S_i^z[\exp(\delta_i/T)]\right\}\Big/\left\{1 + \nu \mathrm{e}^{-\Delta/T}\sum_i \exp(\delta_i/T)\right\}, \tag{9}$$

where S_i^z is the projection of S on the external magnetic field $\mathbf{H}$, $\delta_i = g\mu_\mathrm{B}S_i^zH$, and Δ is either Δ_I or Δ_H. We use the spin-only value $g = 2$, the sum is over $S(S+1)$ levels i, and ν is the degeneracy of the magnetic state. In the model studied in [10] the IS state has ordered e_g orbitals $(x^2\text{–}z^2)^\uparrow$ and $(y^2\text{–}z^2)^\uparrow$ (see figure 6 in [10]) with the t_{2g} hole in the $(xz)^\downarrow$ and $(yz)^\downarrow$

orbitals; $\nu = 3$ (triply degenerate t_{2g} orbital). In the HS state, on the other hand, both e_g levels and two of the three t_{2g} levels are occupied; again $\nu = 3$. (The five-fold S_z degeneracy leading to $\nu = 15$ in [6] is lifted by the field.)

The field of 5.8 T corresponds to $\delta = 7.80$ K. Putting this value of δ and m (100 K) $= 0.09(1)\ \mu_B$ (8) in equation (9) one obtains $\Delta_I = 32^{+115}_{-32}$ and $\Delta_H = 430^{+34}_{-20}$, at $T = 100$ K. The superscripts and subscripts give the estimated standard deviations. In spite of very high uncertainty in Δ_I, its value shows clearly that it is the IS state which is excited at $T \approx 100$ K. Actually Δ_H determined from m (285 K), which should be more sensitive to Δ_H, is even higher. We estimate it as $\Delta_H \approx 1000$ K, a value obtained without correction for the IS contribution which is difficult to calculate because of the large uncertainty in Δ_I.

A statistically significant (99.7% confidence) negative moment $m(O^{2-}) = -0.021(7)\ \mu_B$ is observed on the ligand O^{2-} at 100 K, which is consistent with the theory [10] that predicts a hole in the oxygen 2p shell with its spin opposite to that of Co^{3+}, as shown in figure 5 of [10]. In addition to the gap value argument, this may be considered confirmation that IS is the first excited state, since the same theory predicts the hole and the Co^{3+} spins to be parallel in the case of the HS state. Unfortunately, the precision of the determination of $m(O^{2-})$ is not sufficient to follow its temperature evolution. Such an improvement might be possible with a larger crystal.

In summary, we have shown, from the gap value obtained from the field-induced magnetic moment on Co^{3+} and by the reverse magnetization induced on O^{2-}, that the spin-state transition at $T \approx 100$ can be identified as a LS $\rightarrow$ IS one.

Acknowledgments

This work was carried out in framework of the INTAS project (grant no 01-0278). We are deeply indebted to INTAS for the grant, which has made this study possible. We are grateful to the project coordinator Professor A Furrer for the fruitful scientific discussions and excellent management. Partial support from the Russian Foundations for Basic Researches (project no. 05-02-17466-a), the State Program on Quantum Macrophysics (10002-25/П-03/040-58/100608), by the grants SS-1671.2003.2, MK-1326.2005.2 and by the NATO grant PST CLG 979369, are acknowledged. Two of us, V P Plakhty and S V Gavrilov, are indebted to ILL for hospitality.

References

[1] Sugano S, Tanabe Y and Kamimura H 1970 *Multiplets of Transition-Metal Ions in Crystals* (New York: Academic)
[2] Bhide V G, Rajoria D S, Rao G R and Rao C N R 1972 *Phys. Rev.* B **6** 1021
[3] Asai K, Gehring P, Chou H and Shirane G 1989 *Phys. Rev.* B **40** 10982
[4] Koehler W C and Wollan E O 1957 *J. Phys. Chem. Solids* **2** 100
[5] Menyuk N, Dwight K and Raccah P M 1967 *J. Phys. Chem. Solids* **28** 549
[6] Asai K, Yokokura O, Nishimori N, Chou H, Tranquada J M, Shirane G, Higuchi S, Okajama Y and Kohn K 1994 *Phys. Rev.* B **50** 3025
[7] Naiman C S, Gilmore R, DiBartolo B, Linz A and Santoro R 1965 *J. Appl. Phys.* **36** 1044
[8] Raccah P M and Goodenough J B 1967 *Phys. Rev.* **155** 932
[9] Thornton G, Tofield B C and Hewat A W 1986 *J. Solid State Chem.* **61** 301
[10] Korotin M A, Ezhov S Yu, Solovyev I V, Anisimov V I, Khomskii D I and Sawatzky G A 1996 *Phys. Rev.* B **54** 5309
[11] Zaanen J, Sawatzsky G A and Allen J W 1985 *Phys. Rev. Lett.* **55** 418
[12] Potze R H, Sawatzky G A and Abbate M 1995 *Phys. Rev.* B **51** 11501
[13] Zobel C, Kreiner M, Bruns D, Baier J, Grüninger M, Lorenz T, Reutler P and Revcolevschi A 2002 *Phys. Rev.* B **66** 020402(R)

[14] Saitoh T, Mizokawa T, Fujimori A, Abbate M, Takeda Y and Takano M 1997 *Phys. Rev.* B **55** 4257
[15] Noguchi S, Kawamata S, Okuda K, Nojiri H and Motokawa M 2002 *Phys. Rev.* B **66** 094404
[16] Asai K, Yoneda A, Yokokura O, Tranquada J M, Shirane G and Kohn K 1998 *J. Phys. Soc. Japan* **67** 290
[17] Radelli P G and Cheong S-W 2002 *Phys. Rev.* B **66** 094408
[18] Yamaguchi S, Okimoto Y and Tokura Y 1997 *Phys. Rev.* B **55** R8666
[19] Maris G, Ren Y, Volotchaev V, Zobel C, Lorenz T and Palstra T T M 2003 *Phys. Rev.* B **67** 224423
[20] Kyômen T, Asaka Y and Itoh M 2003 *Phys. Rev.* B **67** 144424
[21] Izyumov Yu A, Naish V E and Ozerov R P 1991 *Neutron Diffraction of Magnetic Materials* (New York: Consultants Bureau)
[22] McCarrol W H, Ramanujachary K V and Greenblatt M 1997 *J. Solid State Chem.* **130** 327
[23] Shirvaev S V, Bychkov G L, Barilo S N, Ustinovich S N, Podlesnyak A, Baran M, Szymczak R and Furrer A 2005 *J. Cryst. Growth* **275** 751
[24] Androulakis J, Katsarakis N and Giapintzakis J 2001 *Phys. Rev.* B **64** 174401
[25] Yan J-Q, Zhou J-S and Goodenough J B 2004 *Phys. Rev.* B **70** 014402
[26] Clementi E and Roetti C 1974 *At. Data Nucl. Data Tables* **14** 177